



CHORUS

This is the accepted manuscript made available via CHORUS. The article has been published as:

Emergent Spinon Dispersion and Symmetry Breaking in Two-Channel Kondo Lattices

Yang Ge and Yashar Komijani

Phys. Rev. Lett. **129**, 077202 — Published 11 August 2022

DOI: [10.1103/PhysRevLett.129.077202](https://doi.org/10.1103/PhysRevLett.129.077202)

Emergent Spinon Dispersion and Symmetry Breaking in Two-channel Kondo Lattices

Yang Ge and Yashar Komijani*

Department of Physics, University of Cincinnati, Cincinnati, Ohio, 45221, USA

(Dated: July 5, 2022)

Two-channel Kondo lattice serves as a model for a growing family of heavy-fermion compounds. We employ dynamical large- N technique and go beyond the independent bath approximation to study this model both numerically and analytically using renormalization group ideas. We show that Kondo effect induces dynamic magnetic correlations that lead to an emergent spinon dispersion. Furthermore, we develop a quantitative framework that interpolates between infinite dimension where the channel-symmetry broken results of mean-field theory are confirmed, and one-dimension where the channel symmetry is restored and a critical fractionalized mode is found.

The screening of a magnetic impurity by the conduction electrons in a metal is governed by the Kondo effect. The multi-channel version is when several channels compete for a single impurity, as a result of which the spin is frustrated and a new critical groundstate formed with a fractional residual impurity entropy. In the two-channel case, this entropy $\frac{1}{2} \log 2$ corresponds to a Majorana fermion. If the channel symmetry is broken, the weaker channels decouple and the stronger-coupled channels *win* to screen the impurity at low temperature [1–4].

While the case of a single impurity is well understood, much less is known about Kondo lattices where a lattice of spins is screened by conduction electrons [5–7], especially if multiple conduction channels are involved [8]. The most established fact is the prediction of a large Fermi surface (FS) in the Kondo-dominated regime of the single-channel Kondo lattice [9]. In the multi-channel case, the continuous channel symmetry naturally leads to new patterns of entanglement which are potentially responsible for the non-Fermi liquid physics [10, 11], symmetry breaking and possibly fractionalized order parameter [12]. This partly arises from the fact that the residual entropy seen in the impurity has to eventually disappear at zero temperature in the case of a lattice.

Beside fundamental interest, a pressing reason for studying this physics is that the multi-channel Kondo lattice (MCKL), and in particular 2CKL, seems to be an appropriate model for several heavy-fermion compounds, e.g. the family of $\text{PrTr}_2\text{Zn}_{20}$ ($\text{Tr}=\text{Ir,Rh}$) [13, 14] as well as recent proposals that MCKLs may support non-trivial topology [15, 16] and non-abelian Kondo anyons [17, 18].

The MCKL model is described by the Hamiltonian

$$H = H_c + J_K \sum_j \vec{S}_j \cdot c_{ja}^\dagger \vec{\sigma} c_{ja} \quad (1)$$

where $H_c = -t_c \sum_{\langle ij \rangle} (c_{i\alpha}^\dagger c_{j\alpha} + h.c.)$ is the Hamiltonian of the conduction electrons and Einstein summation over spin $\alpha, \beta = 1 \dots N$ and channel $a, b = 1 \dots K$ indices is assumed. This model has $\text{SU}(N)$ spin and $\text{SU}(K)$ channel symmetries and we are interested to analyze the effect of a channel (ch.) symmetry breaking $H \rightarrow H + \sum_j \Delta \vec{J}_j \cdot \vec{O}_j$, where $\vec{O}_j \equiv (\vec{S}_j \cdot c_{ja}^\dagger \vec{\sigma} c_{jb}) \vec{\tau}_{ba}$ and $\vec{\tau}$ -s act as Pauli matrices in the channel space [19]. At first look, at least

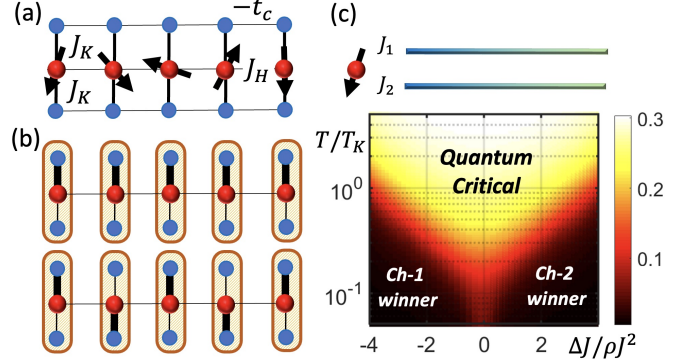


FIG. 1. (a) The 1D version of the two-channel Kondo lattice model studied here. (b) The strong coupling leads to a channel magnet; two different patterns of channel symmetry breaking, ch. FM (top) and ch. AFM (bottom). Bold lines represents spin-singlets. (c) The entropy S of two-channel Kondo impurity vs. ch. asymmetry and temperature. At the symmetric point, S reduces to a fraction of the high- T value.

certain deformation [20] of the MCKL can be thought of as a channel magnet. In the $J_K \rightarrow \infty$ limit [21], the spin is quenched due to formation of Kondo singlet with either (for $K = 2$) of the channels, leading to a doublet over which \vec{O} acts like $\vec{\tau}$ [21, 22]. Interaction among adjacent doublets leads to a “channel magnet” $H_{\text{eff}} \propto \frac{t^2}{J_K} \sum_{\langle ij \rangle} \vec{O}_i \cdot \vec{O}_j$. While channel Weiss-field favors a ch. anti-ferromagnetic (ch. AFM) super-exchange interaction, the mean-field theory predicts a variety of ch. ferromagnetic (ch. FM) and ch. AFM solutions [Fig. 1(b)] depending on the conduction filling.

On the other hand, some differences to a channel magnet are expected since the winning channel has a larger FS [12, 23] and the order parameter \vec{O} is strongly dissipated by coupling to fermionic degrees of freedom. Although a channel-symmetry broken groundstate is predicted by both single-site dynamical mean-field theory (DMFT) [19, 24] and static mean-field theory [23, 25, 26], it has not been observed in recent cluster DMFT studies [27]. Furthermore, the effective theory of fluctuations in the large- N limit [23] predicts a disordered phase below the lower critical dimension but the nature of this quan-

tum paramagnet is unclear. In 1D, Andrei and Orignac have used non-abelian bosonization to show [28] that the groundstate is gapless and fractionalized (dispersing Majoranas for $K = 2$), a prediction that contradicts the analysis by Emery and Kivelson [29], and has *not* been confirmed by the density matrix renormalization group calculations [22].

Resolving these issues requires a technique that is applicable to arbitrary dimensions and goes beyond static mean-field and DMFT by capturing both quantum and spatial fluctuations. Here we show that dynamical large- N approach, recently applied successfully to study Kondo lattices [18, 30–37], is precisely such a technique.

We assume the spins transform as a spin- S representation of $SU(N)$. In the impurity case [38], the spin is fully screened for $K = 2S$ whereas it is over/under-screened for $K > 2S$ and $K < 2S$, respectively [39]. The focus of this paper is on the Kondo-dominated regime of the double-screened case $K/2S = 2$ which is schematically shown in Fig. 1(a). We use Schwinger bosons $S_{j\alpha\beta} = b_{j\alpha}^\dagger b_{j\beta}$ to form a symmetric representation of spins with the size $2S = b_{j\alpha}^\dagger b_{j\alpha}$. We then re-scale $J_K \rightarrow J_K/N$ and treat the model (1) in the large- N limit, by sending $N, K, S \rightarrow \infty$, but keeping $s = S/N$ and $\gamma = K/N = 4s$ constant. The constraint is imposed on average via a uniform Lagrange multiplier μ_b .

In the present large- N limit, the RKKY interaction is $O(1/N)$ [inset of Fig. 2(a)] and we need to include an explicit Heisenberg interaction $H \rightarrow H + J_H \sum_{\langle ij \rangle} \vec{S}_i \cdot \vec{S}_j$ between nearest neighbors $\langle ij \rangle$ to couple the impurities. Nevertheless, we will show that an infinitesimal J_H is sufficient to produce significant magnetic correlations due to a novel variant of RKKY interaction. For simplicity we limit ourselves to ferromagnetic correlations $J_H < 0$.

For a \mathcal{V} site lattice, the Lagrangian becomes [31, 40]

$$\mathcal{L} = \sum_k \bar{c}_{ka\alpha} (\partial_\tau + \epsilon_k) c_{ka\alpha} + \sum_k \bar{b}_{k\alpha} (\partial_\tau + \epsilon_k) b_{k\alpha} \quad (2)$$

$$+ \sum_j \frac{\bar{\chi}_{ja} \chi_{ja}}{J_K} + \sum_j \frac{1}{\sqrt{N}} (\bar{\chi}_{ja} b_{j\alpha} \bar{c}_{j\alpha} + h.c.) + 2\mathcal{V} \mu_b S.$$

Here, b -s are bosonic spinons and χ -s are Grassmannian holons that mediate the local Kondo interaction. In momentum space, the electrons and bosons have dispersions $\epsilon_k = -2t_c \cos k - \mu_c$ and $\epsilon_k = -2t_b \cos k - \mu_b$, respectively. t_b is the (assumed to be homogeneous) nearest neighbor hopping of spinons due to large- N decoupling of J_H term [31]. Here, we focus on a half-filled conduction band $\mu_c = 0$, but similar results are obtained at other commensurate fillings [21]. In the large- N limit the dynamics is dominated by the non-crossing Feynman diagrams, resulting in boson and holon self-energies [$\vec{r} \equiv (j, \tau)$]

$$\Sigma_b(\vec{r}) = -\gamma G_c(\vec{r}) G_\chi(\vec{r}), \quad \Sigma_\chi(\vec{r}) = G_c(-\vec{r}) G_b(\vec{r}), \quad (3)$$

whereas Σ_c is $O(1/N)$ and thus the electrons propagator $G_c^{-1}(k, z) = z - \epsilon_k$ remains bare, with z complex

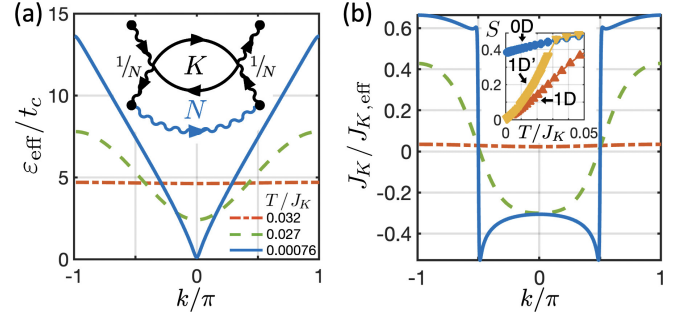


FIG. 2. 1D 2CKL model. The temperature evolution of (a) the effective energy ϵ_{eff} for spinons and (b) the inverse effective Kondo coupling $J_{K,\text{eff}}^{-1}$ for holons. At high- T , $J_{K,\text{eff}} = J_K$ with no k dependence. Initially, Kondo effect develops locally and $J_{K,\text{eff}}^{-1} \rightarrow 0$. Then dispersion emerges in both G_χ and G_b , with $J_{K,\text{eff}}^{-1}$ vanishing only at $k \sim \pm k_F$ and ϵ_{eff} only at $k \sim 0$. Inset of (a): Despite an $O(1/N)$ RKKY interaction (black), an initial spinon dispersion (blue) can lead to an $O(1)$ amplification to in the present over-screened case. Inset of (b): Entropy S vs. T for 0D, 1D ($t_b = 0.2t_c$) and 1D' ($t_b = 0.0002t_c$).

frequency. Eqs. (3) together with the Dyson equations $G_b^{-1}(k, z) = z - \epsilon_k - \Sigma_b(k, z)$ and $G_\chi^{-1}(k, z) = -J_{K,a}^{-1} - \Sigma_\chi(k, z)$ form a set of coupled integral equations that are solved iteratively and self-consistently, while μ_b is adjusted to satisfy the constraint. Thermodynamic variables are then computed from Green's functions [30, 31].

First, we study the case in which J_H is absent, or $\epsilon_k = -\mu_b$. In this limit, the self-energies remain local $\Sigma_{b,\chi}(n, \tau) \rightarrow \delta_{n0} \Sigma_{b,\chi}(\tau)$ and the problem reduces to the impurity problem [40]. It has never been studied whether the large- N over-screened impurities are susceptible to symmetry breaking [2]. To do so, we assume that half of K channels are coupled to the impurity with $J_K + \Delta J$ and the other half with $J_K - \Delta J$. This corresponds to a uniform symmetry breaking deformation $\Delta \mathcal{L} = (\Delta J/J_K^2) \sum_j [\bar{\chi}_{j1} \chi_{j1} - \bar{\chi}_{j2} \chi_{j2}]$ of the Lagrangian. Fig. 1(c) shows the entropy of the 2CK impurity model as a function of channel asymmetry, verifying that the impurity is indeed critical w.r.t. channel symmetry breaking. In symmetric 2CK, the ground state entropy at large- N is fractional with a universal dependence on (γ, s) [21, 40].

Next, we focus on finite t_b case for two settings of 1D and ∞ D, which correspond to a Bethe lattice with coordination numbers $z = 2$ and $z = \infty$. In 1D, $G(k, z)$ and $\Sigma(k, z)$ depend on k and z , but in ∞ D, self-energies have no spatial dependence and the Green's functions of spinons/electrons obey $G_{b,c}^{-1} = z + \mu_{b,c} - \Sigma_{b,c}(z) - t_{b,c}^2 G_{b,c}$.

Importantly, the criticality of over-screened impurity solution ensures that an infinitesimal spinon hopping seed $t_b \sim 0$ can get an $O(1)$ amplification [inset of Fig. 2(a)] and dispersions for spinons and holons are *dynamically* generated. Restricting ourselves to translationally invariant solutions with lattice periodicity a ,

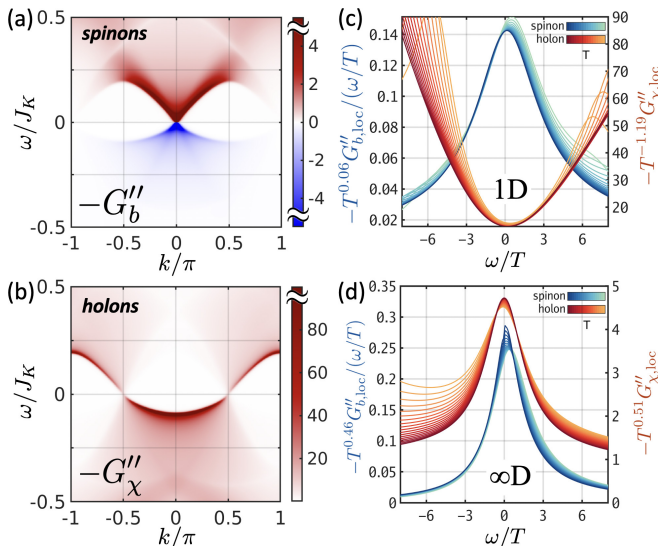


FIG. 3. The spectral function of (a) spinons and (b) holons in a 1D two-channel Kondo lattice at $T/J_K = 0.0072$, showing emergent linearly-dispersing spinons at $k = 0$ (bare dispersion is quadratic) and holons with Fermi point at $\pm k_F$. Scaling collapse of spinon and holon Green's functions in the 2CK critical regime in (c) 1D lattice ($z = 2$) $0.0072 \leq T/J_K \leq 0.03$ and (d) ∞ D Bethe lattice ($z = \infty$) $0.006 \leq T/J_K \leq 0.03$. For both cases, $J_K/t_c = 6$, $t_b/t_c = 0.2$, and $s = 0.15$.

149 this effect can be succinctly represented by the zero-
150 frequency spinon/holon effective dispersion $J_{K,\text{eff}}^{-1}(k) \equiv$
151 $-\text{Re}[G_\chi^{-1}(k, \omega = 0)]$ and $\varepsilon_{\text{eff}}(k) \equiv -\text{Re}[G_b^{-1}(k, \omega = 0)]$,
152 shown in Fig. 2(a,b) for various temperatures. This emer-
153 gent spinon dispersion is independent of the choice of the
154 seed and agrees qualitatively with the finite t_b results [21].
155 The consumption of the residual entropy in the lattice by
156 the emerging dispersion is visible in the inset of Fig. 2(b).
157 We stress that in 1D, this apparent transition most likely
158 becomes a crossover when N is finite [41]. In the case of
159 ∞ D, the system is prone to spin or channel magnetiza-
160 tion, as discussed later. Such symmetry breakings would
161 consume the residue entropy [21].

162 Fig. 3(a,b) shows the finite frequency spectral func-
163 tion of spinons and holons, respectively. Both are domi-
164 nated by a sharp mode with emergent Lorentz invariance.
165 The spinons are gapless and linearly dispersing and the
166 holons form a FS. The temperature collapse of Fig. 3(c)
167 confirms that the spectra are critical with the local spec-
168 tra obeying a $T^{1-2\Delta_{b,\chi}} G''_{b,\chi}(x = 0, \omega) = f_{b,\chi}(\omega/T)$ be-
169 havior. Fig. 3(d) shows similar collapse for the case of
170 infinite-coordination Bethe lattice (∞ D). A marked dif-
171 ference between the two cases is that $\Delta_\chi > 1/2$ for 1D,
172 which leads to $-G''_\chi$ minima at $\omega \sim 0$, whereas $\Delta_\chi < 1/2$
173 in ∞ D, manifested as a peak at $\omega \sim 0$.

174 What is the effect of channel symmetry breaking
175 on the volume of FS? According to Luttinger's theo-
176 rem, the FS volume is related to electron phase shift
177 $v_a^{\text{FS}} = \mathcal{V}^{-1} \sum_k \delta_a(k)$ for a d dimensional lattice. From

178 $K = 4S$ case of the Ward identity [42], the electron
179 phase shift is related to that of holons $N\delta_{c,a}(k) = \delta_{\chi,a}(k)$,
180 which itself is defined as

$$\delta_{\chi,a}(k) = -\text{Im}\{\text{log}[-G_{\chi,a}^{-1}(k, 0 + i\eta)]\}. \quad (4)$$

181 In 1D, holons are occupied for $|k| < \pi/2$. The locus of
182 points at which $J_{K,\text{eff}}^{-1}(k)$ changes sign defines a holon
183 FS which generalizes to any dimension. So, we find that
184 $v_{\chi,a}^{\text{FS}} = 2\pi S/K = \pi/2$ and the total change in electron
185 FS is $N\Delta v_{c,a}^{\text{FS}} = \pi/2$, corresponding to a large FS in the
186 critical phase. We use Eq. (4) to study the effect of a uni-
187 form symmetry breaking field $\Delta\mathcal{L}$. Fig. 4(a) shows how
188 FSs of slightly favored and disfavored channels evolve as
189 a function of T in the two cases. In 1D, the FS asym-
190 metry disappears, restoring a ch. symmetric criticality at
191 low T , consistent with the Mermin-Wagner theorem. On
192 the other hand, in ∞ D the asymmetry grows and one
193 channel totally decouples from the spins, with gapped
194 spinons and holons for both channels. The exponents
195 are related to Δ_χ ; varying ΔJ in Eq. (4) we find

$$\frac{\partial v_{\chi,a}^{\text{FS}}}{\partial \Delta J} = \frac{-1}{\mathcal{V}} \sum_k G''_\chi(k, 0 + i\eta) = -G''_\chi(x = 0, 0 + i\eta). \quad (5)$$

196 Assuming $|G_\chi(\vec{r})| \sim |\vec{r}|^{-2\Delta_\chi}$, the holon FS is unsta-
197 ble against symmetry breaking when $G''_\chi(k_F, 0 + i\eta) \sim$
198 $T^{2\Delta_\chi - d - 1}$ diverges. This $2\Delta_\chi < d + 1$ regime coincides
199 with when the symmetry breaking term ΔJ is relevant,
200 in the renormalization group (RG) sense. On the other
201 hand instability of the entire holon FS requires the diver-
202 gence of $G''_\chi(x = 0, 0 + i\eta) \sim T^{2\Delta_\chi - 1}$, i.e. $2\Delta_\chi < 1$ which
203 is a more stringent condition and agrees with Fig. 4(a),
204 confirming $\Delta_\chi = 1/2$ as the marginal dimension.

205 Fig. 4(a) shows that the symmetry breaking $\Delta\mathcal{L}$ is
206 relevant in ∞ D, but is irrelevant in 1D. To establish this
207 from the microscopic model, one has to access the in-
208 frared (IR) fixed point. From the numerics we see that
209 the system flows to a critical IR fixed point, in which
210 spinons and holons are critical in addition to electrons.
211 For an impurity $G_b \sim |\tau|^{-2\Delta_b}$ and $G_\chi(\tau) \sim |\tau|^{-2\Delta_\chi}$ are
212 reasonable at $T = 0$. The exponents are known [21, 40]:

$$0, \infty\text{D} : \quad \Delta_\chi = \frac{\gamma}{2(1 + \gamma)}, \quad \Delta_b = \frac{1}{2(1 + \gamma)}, \quad (6)$$

213 and coincide with those of the ∞ D in the small t_b regime
214 we are interested here [21]. In presence of a dimensionless
215 $\lambda_0 = \Delta J/\rho J_K^2$, the RG analysis $d\lambda/d\ell = (1 - 2\Delta_\chi)\lambda$
216 predicts a dynamical scale $w \sim T_K \lambda_0^{1+\gamma}$ [c.f. Fig. 1(c)].

217 The 1D case is more subtle; as $T \rightarrow 0$, we see from
218 Fig. 2 that $J_{K,\text{eff}}^{-1}(\pm k_F) \rightarrow 0$ and $\varepsilon_{\text{eff}}(0) \rightarrow 0$ at the IR
219 fixed point [43]. This means that the Kondo coupling
220 flows to strong coupling at $|k| < k_F$, to weak coupling at
221 $|k| > k_F$, and gets critical at $k = \pm k_F$, while the spinons
222 are gapless at $k = 0$. At these momenta, the Dyson equa-
223 tion has the form $G_b \Delta \Sigma_b|_{k \sim 0} = G_\chi \Delta \Sigma_\chi|_{k \sim \pm k_F} = -1$.

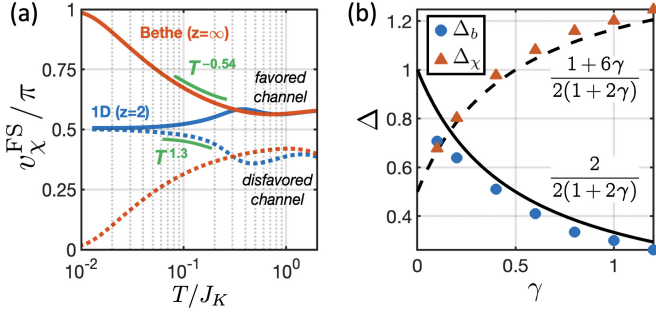


FIG. 4. (a) The evolution of FS in presence of small channel symmetry breaking in 1D and ∞ D with temperature. (b) The scaling exponents $\Delta_{b/\chi}$ in 1D from the numerics. The lines show the analytical values given by Eqs. (9).

We can obtain a low-energy description by expanding fields near zero energy, e.g. $\psi(x) \sim e^{ik_F x} \psi_R + e^{-ik_F x} \psi_L$ for electrons and holons. In 1+1 dimensions, the conformal invariance of the fixed point dictates the following form for the $T = 0$ Green's functions $G(x, \tau) = G(z, \bar{z})$:

$$G_b = -\bar{\rho} \left(\frac{a^2}{\bar{z}z} \right)^{\Delta_b}, \quad G_{\chi R/L} = \frac{-1}{2\pi} \left(\frac{a}{\bar{z}} \right)^{\Delta_x \pm \frac{1}{2}} \left(\frac{a}{z} \right)^{\Delta_x \mp \frac{1}{2}} \quad (7)$$

where $z = v\tau + ix$ and $\bar{\rho} = 2s/a$. The $G_{cR/L}$ is obtained from $G_{\chi R/L}$ by $\Delta_{\chi} \rightarrow 1/2$. These Green's functions can be conformally mapped to finite- T via $z \rightarrow (\beta/\pi) \sin(\pi z/\beta)$ replacement. Furthermore, in terms of $q = k + i\omega/v$, they have the Fourier transforms:

$$G_b = -2\pi a^2 \bar{\rho} v_b^{-1} (a^2 \bar{q}q)^{\Delta_b - 1} \zeta_0(\Delta_b) \quad (8)$$

$$G_{\chi R/L} = \mp a^2 v_{\chi}^{-1} (a\bar{q})^{\Delta_x - 1 \mp 1/2} (aq)^{\Delta_x - 1 \pm 1/2} \zeta_1(\Delta_{\chi})$$

where $\zeta_n(\Delta) \equiv 2^{1-2\Delta} \Gamma(1 - \Delta + n/2) / \Gamma(n/2 + \Delta)$. From matching the powers of frequency in Eqs. (3,7,8), we conclude that $\Delta_b + \Delta_{\chi} = 3/2$ in order to satisfy the self-consistency. Moreover, from the matching of the amplitude of the Green's functions we find [21]

$$1D: \quad \Delta_{\chi} = \frac{1+6\gamma}{2(1+2\gamma)}, \quad \Delta_b = \frac{2}{2(1+2\gamma)}. \quad (9)$$

Note that $\Delta_{\chi} > 1/2$, ensuring that channel symmetry breaking perturbations are irrelevant in 1D. These are in excellent agreement with the exponents extracted from ω/T scaling [Fig. 4(b)] and we have established a semi-analytical framework to interpolate between 1D and ∞ D.

The emergent dispersion in Fig. 2, the scaling dimensions in Eq. (9) and their relation to symmetry breaking in Fig. 4 are the central results of this paper. In the following we discuss some of the implications of these results for physical observables that are independent of our fractionalized description, leaving the details to [21].

The fractionalization $S_{\alpha\beta} \sim b_{\alpha}^{\dagger} b_{\beta}$ or $b_{\alpha}^{\dagger} c_{\alpha\alpha} \sim \chi_a$ contraction are related to order parameter fractionalization [12, 44]. In the long time/distance limit, correlation functions of $b_{\alpha}^{\dagger} c_{\alpha\alpha}$ and that of χ_a are given by Σ_{χ} and

G_{χ} , respectively and thus, have exponents that add up to zero. On the other hand, correlators of gauge-invariant operators $\mathcal{X}_{ab} \equiv \bar{\chi}_a \chi_b$ and $\mathcal{O}_{ab} \equiv b_{\alpha}^{\dagger} b_{\beta} c_{\beta\beta}^{\dagger} c_{\alpha\alpha}$ are exactly equal since both can be constructed by taking derivatives of free energy w.r.t. ΔJ^{ab} before/after Hubbard-Stratonovitch transformation. A diagrammatic proof of this equivalence is provided in [21]. Scaling analysis gives $\chi_{\text{ch}}(x=0) \sim T^{4\Delta_{\chi}-1}$ and $\chi_{\text{ch}}^{\text{1D}}(q=0) \sim T^{4\Delta_{\chi}-2}$ up to a constant shift coming from the regular part of free energy.

Another non-trivial feature of 2CK impurity fixed point is its magnetic instability [2] whose large- N incarnation is $\Delta_b < 1/2$ for the impurity (or ∞ D) in Eq. (6). From Eq. (9), we see that this also holds for 1D 2CKL for $\gamma > 1/2$. This is reflected in the divergence of the uniform $\chi_m(q=0)$ static magnetic susceptibilities as a function of T . Using scaling analysis $\chi_m^{\text{1D}}(q=0) \sim T^{4\Delta_b-2}$ and $\chi_m(x=0) \sim T^{4\Delta_b-1}$ up to a constant shift, in good agreement with numerics [21]. Note that this critical spin behavior is different from the gapped spin sector observed in [22, 29], but is qualitatively consistent with [28].

Lastly, the fact that the fixed point discussed above is IR stable follows from the fact that the interaction is exactly marginal due to $\Delta_b + \Delta_{\chi} = 3/2$ and that vertex corrections remain $O(1/N)$. The 1+1D correlators (7) can be obtained from three sets of decoupled Luttinger liquids for each of the c, b, χ fields with fine-tuned Luttinger parameters that give the correct exponents. Such a spinon-holon theory will have a Virasoro central charge $c_0/N = 1 + \gamma$. On the other hand the coset theory of [21, 28, 45] predicts $c_{AO}/N = \gamma/(1 + \gamma)$. We have used $T \rightarrow 0$ heat-capacity and the excitation velocities v to compute the central charge according to $C/T = (\pi k_B^2/6v)c$ as a function of γ and found $c = c_0$ [21]. Note that there is no contradiction with c-theorem since the UV theory is not Lorentz invariant due to ferromagnetism. The discrepancy with c_{AO} is likely rooted in inability of Schwinger bosons to capture gapless spin-liquids [46].

In summary, we have shown that dynamical large- N approach can capture symmetry breaking in multi-channel Kondo impurities and lattices in presence of both emergent and induced ferromagnetic correlations within an RG framework with explicit examples on 0D, 1D and ∞ D. The scaling analysis enables an analytical solution to the critical exponents and susceptibilities which are in good quantitative agreement with numerics, and is applicable to higher dimensional CFTs. A determination of upper/lower critical dimensions and effect of anti-ferromagnetic correlation is left to a future work [47].

Acknowledgment—The authors acknowledge fruitful discussions with P. Coleman and N. Andrei. This work was performed in part at Aspen Center for Physics, which is supported by NSF grant PHY-1607611. Computations for this research were performed on the Advanced Research Computing center at the University of Cincinnati, and the Penn State University's Institute for Computa-

310 tional and Data Sciences' Roar supercomputer.

-
- 311 [1] N. Andrei and C. Destri, *Phys. Rev. Lett.* **52**, 364 (1984).
 312 [2] I. Affleck, A. W. W. Ludwig, H.-B. Pang, and D. L. Cox,
 313 *Phys. Rev. B* **45**, 7918 (1992).
 314 [3] V. J. Emery and S. Kivelson, *Phys. Rev. B* **46**, 10812
 315 (1992).
 316 [4] I. Affleck and A. W. W. Ludwig, *Phys. Rev. B* **48**, 7297
 317 (1993).
 318 [5] A. C. Hewson, *The Kondo Problem to Heavy Fermions*,
 319 Cambridge Studies in Magnetism (Cambridge University
 320 Press, 1993).
 321 [6] Q. Si, J. H. Pixley, E. Nica, S. J. Yamamoto, P. Goswami,
 322 R. Yu, and S. Kirchner, *J. Phys. Soc. Jpn.* **83**, 061005
 323 (2014).
 324 [7] P. Coleman, *Introduction to Many-Body Physics* (Cam-
 325 bridge University Press, 2015).
 326 [8] D. L. Cox and M. Jarrell, *J. Phys. Condens. Matter* **8**,
 327 9825 (1996).
 328 [9] M. Oshikawa, *Phys. Rev. Lett.* **84**, 3370 (2000).
 329 [10] M. Jarrell, H. Pang, D. L. Cox, and K. H. Luk, *Phys.*
 330 *Rev. Lett.* **77**, 1612 (1996).
 331 [11] M. Jarrell, H. B. Pang, and D. L. Cox, *Phys. Rev. Lett.*
 332 **78**, 1996 (1997).
 333 [12] Y. Komijani, A. Toth, P. Chandra, and P. Coleman,
 334 [arXiv:1811.11115](https://arxiv.org/abs/1811.11115) (2018).
 335 [13] T. Onimaru and H. Kusunose, *J. Phys. Soc. Jpn.* **85**,
 336 082002 (2019).
 337 [14] A. S. Patri and Y. B. Kim, *Phys. Rev. X* **10**, 041021
 338 (2020).
 339 [15] H. Hu, L. Chen, C. Setty, S. E. Grefe, A. Prokofiev,
 340 S. Kirchner, S. Paschen, J. Cano, and Q. Si,
 341 [arXiv:2110.06182](https://arxiv.org/abs/2110.06182) (2021).
 342 [16] M. Kornjaca, V. L. Quito, and F. Rebecca,
 343 [arXiv:2104.11173](https://arxiv.org/abs/2104.11173) (2021).
 344 [17] P. L. S. Lopes, I. Affleck, and E. Sela, *Phys. Rev. B* **101**,
 345 085141 (2020).
 346 [18] Y. Komijani, *Phys. Rev. B* **101**, 235131 (2020).
 347 [19] S. Hoshino, J. Otsuki, and Y. Kuramoto, *Phys. Rev.*
 348 *Lett.* **107**, 247202 (2011).
 349 [20] A naïve strong coupling limit is not a spin-singlet, but
 350 the Nozières doublet. See the supplementary material for
 351 a deformation that changes this.
 352 [21] See supplementary materials.
 353 [22] T. Schauerte, D. L. Cox, R. M. Noack, P. G. J. van Don-
 354 gen, and C. D. Batista, *Phys. Rev. Lett.* **94**, 147201
 355 (2005).
 356 [23] A. Wugalter, Y. Komijani, and P. Coleman, *Phys. Rev.*
 357 *B* **101**, 075133 (2020).
 358 [24] S. Hoshino and Y. Kuramoto, *J. Phys. Conf. Ser.* **592**,
 359 012098 (2015).
 360 [25] J. S. Van Dyke, G. Zhang, and R. Flint, *Phys. Rev. B*
 361 **100**, 205122 (2019).
 362 [26] G. Zhang, J. S. Van Dyke, and R. Flint, *Phys. Rev. B*
 363 **98**, 235143 (2018).
 364 [27] K. Inui and Y. Motome, *Phys. Rev. B* **102**, 155126
 365 (2020).
 366 [28] N. Andrei and E. Orignac, *Phys. Rev. B* **62**, R3596
 367 (2000).
 368 [29] V. J. Emery and S. A. Kivelson, *Phys. Rev. Lett.* **71**,
 369 3701 (1993).
 370 [30] J. Rech, P. Coleman, G. Zarand, and O. Parcollet, *Phys.*
 371 *Rev. Lett.* **96**, 016601 (2006).
 372 [31] Y. Komijani and P. Coleman, *Phys. Rev. Lett.* **120**,
 373 157206 (2018).
 374 [32] Y. Komijani and P. Coleman, *Phys. Rev. Lett.* **122**,
 375 217001 (2019).
 376 [33] J. Wang, Y.-Y. Chang, C.-Y. Mou, S. Kirchner, and
 377 C.-H. Chung, *Phys. Rev. B* **102**, 115133 (2020).
 378 [34] B. Shen, Y. Zhang, Y. Komijani, M. Nicklas, R. Borth,
 379 A. Wang, Y. Chen, Z. Nie, R. Li, X. Lu, *et al.*, *Nature*
 380 **579**, 51 (2020).
 381 [35] J. Wang and Y.-f. Yang, *Phys. Rev. B* **104**, 165120
 382 (2021).
 383 [36] V. Drouin-Touchette, E. J. König, Y. Komijani, and
 384 P. Coleman, *Phys. Rev. B* **103**, 205147 (2021).
 385 [37] R. Han, D. Hu, J. Wang, and Y.-f. Yang, *Phys. Rev. B*
 386 **104**, 245132 (2021).
 387 [38] We use 0D to refer to the impurity problem, although a
 388 conduction band exists.
 389 [39] P. Zinn-Justin and N. Andrei, *Nucl. Phys. B* **528**, 648
 390 (1998).
 391 [40] O. Parcollet and A. Georges, *Phys. Rev. Lett.* **79**, 4665
 392 (1997).
 393 [41] N. Read, *Journal of Physics C: Solid State Physics* **18**,
 394 2651 (1985).
 395 [42] P. Coleman, I. Paul, and J. Rech, *Phys. Rev. B* **72**,
 396 094430 (2005).
 397 [43] This is not the case for the spinon's π -mode, $\epsilon_{\text{eff}}(\pm\pi/a) \neq$
 398 0, but this mode has negligible spectral weight.
 399 [44] A. M. Tsvetlik and P. Coleman, [arXiv:2112.07781](https://arxiv.org/abs/2112.07781) (2021).
 400 [45] P. Azaria, P. Lecheminant, and A. A. Nersisyan, *Phys-*
 401 *ical Review B* **58**, R8881 (1998).
 402 [46] D. P. Arovas and A. Auerbach, *Phys. Rev. B* **38**, 316
 403 (1988).
 404 [47] Y. Ge and Y. Komijani, in preparation.